Open Access Full Text Article

ORIGINAL RESEARCH

# Overexpression of ATF4 Inhibits Ferroptosis to Alleviate Anxiety Disorders by Activating the TGF-β Signaling Pathway

Wentao Wu[1,]*, Fei Wen[1,]*, Jiaxin Hu[1], Leijun Li [2]

[1]Department of Psychiatry, The Second Affiliated Hospital of Guangzhou Medical University, Guangzhou City, Guangdong Province, People's Republic of China; [2]Department of Psychiatry, The Third Affiliated Hospital, Sun Yat-Sen University, Guangzhou City, Guangdong Province, People's Republic of China

*These authors contributed equally to this work

Correspondence: Leijun Li, Email lljzssyxl@163.com

**Background:** Anxiety disorders seriously impair patients' mental health and quality of life, with limited effectiveness of current treatments. Dysregulation of activating transcription factor 4 (ATF4) is involved in various mental diseases, but the research on its potential roles in alleviating anxiety disorders remains limited.

**Methods:** ATF4 was screened out by bioinformatic analysis and its expression was verified in vivo. Mice were treated with 21 d of chronic restraint stress to establish the anxiety mice model. The anxiolytic effect of ATF4 was assessed by a battery of behavior tests and evaluation of hippocampal tissue damage after overexpressing ATF4. Ferroptosis-related indicators were detected by enzyme-linked immunosorbent assay and Western blotting. Then the transforming growth factor beta (TGF-β) signaling pathway was predicted as the downstream regulatory pathway of ATF4 by bioinformatic methods. Western blotting was conducted to detect the protein expression level of TGF-β1, small mothers against decapentaplegic 3 (Smad3), and phospho-Smad3 (p-Smad3).

**Results:** ATF4 was screened out as a ferroptosis-related anxiolytic gene after bioinformatics analysis and was down-regulated in the anxiety mice model. Mice with ATF4 overexpression spent more time in the open arms in the elevated plus-maze test, appeared more frequently in the central area in the open-field test, and decreased the immobility time in the forced swimming and tail suspension tests. Hippocampal tissue damage was alleviated, ferroptosis was suppressed, and the levels of TGF-β1 and p-Smad3/Smad3 were increased by AFT4 overexpression.

**Conclusion:** ATF4 overexpression can repress ferroptosis to improve anxiety disorders by activating the TGF-β signaling pathway.

**Keywords:** anxiety disorders, ATF4, ferroptosis, hippocampus, TGF-β signaling pathway

## Introduction

Anxiety disorders, one of the most widespread mental diseases, can cause a series of symptoms including insomnia, cognitive impairment, irritability, and social impairment,[1–3] with significant impairment of the lives of patients.[4] At present, pharmacotherapy and psychotherapy are the main treatments for anxiety disorders.[3] Nevertheless, there are some limitations of the above approaches because of drug adverse effects and the poor therapeutic effect of psychotherapy.[5] Hence, it is of great importance to find novel therapies for anxiety disorders with fewer adverse effects and higher efficacy.

Ferroptosis, a non-caspase-dependent type of programmed cell death, is driven by the accumulated level of intracellular ferrous iron and lipid peroxidation.[6] During the occurrence of ferroptosis, the excessively accumulated intracellular ferrous iron activates the Fenton reaction to elevate the expression level of hydroxyl radical accompanied by lipid peroxidation and ultimately contributes to cell membrane rupture and cell death.[7] Xu et al have found that ferroptosis is involved in the pathogenesis of alcohol exposure-induced anxiety.[8] Inducing ferroptosis promotes lipopolysaccharide-induced cognitive dysfunction and aggravates anxiety-like behaviors.[9] Suppression of ferroptosis can alleviate the anxiety-like and depressive-like behaviors of type 1 diabetic mice.[10] The above reports indicate the

important role of ferroptosis in anxiety disorders. Hence, it is meaningful to search for therapeutic targets for anxiety disorders based on the regulatory mechanism of ferroptosis.

Activating transcription factor 4 (ATF4), a member of the activating transcription factor/cyclic adenosine monophosphate response element-binding family, is involved in many physiological processes, including ferroptosis.[11] Based on the role of regulating ferroptosis, ATF4 is found to take part in the progression of various kinds of cancer,[12–14] angiogenesis,[15] atherosclerosis,[16] etc. In addition, dysregulation of ATF4 has been considered to be associated with various mental diseases, such as Parkinson's disease,[17] Alzheimer's disease,[18] and depression.[19] Yuan et al have reported that overexpression of ATF4 in the colon can improve stress-related behavioral alterations in mice.[19] Down-regulation of ATF4 can elevate neuronal excitability by regulating the γ-aminobutyric acid type B receptors.[20] Additional research has reported that ATF4 suppression impairs memory and behavioral flexibility.[21] Nevertheless, knowledge of its potential roles in alleviating anxiety disorders remains limited.

In this research, ATF4, significantly down-regulated in anxiety samples, was considered a key ferroptosis-related differentially expressed gene (DEG) by bioinformatics analysis. Then we investigated the potential effect of ATF4 on anxiety and found that overexpression of ATF4 could alleviate chronic restraint stress (CRS)-induced anxiety of mice via inhibiting ferroptosis of hippocampal neurons and up-regulating the expression levels of key proteins of the transforming growth factor beta (TGF-β) pathway, which we hope to provide more insights into exploring novel therapeutic target for anxiety disorders.

## Materials and Methods

### Data Sources and Preprocessing

Firstly, to collect the original gene expression profiles, we downloaded a related microarray dataset, GSE8641, from the Gene Expression Omnibus (GEO) database (https://www.ncbi.nih.gov/geo/) after screening using "Anxiety" as the search query. A total of 12 samples, including 6 anxiety samples and 6 control samples, were selected for the following analysis. A boxplot was drawn to conduct data correction and standardization of selected samples. In addition, we acquired the ferroptosis-related genes (FRGs) from the GeneCards database (https://www.genecards.org).

The online tool GEO2R (https://www.ncbi.nlm.nih.gov/geo/geo2r) was used to identify the DEGs (Anxiety vs Control) which met adjusted $p$-value < 0.05 and $|\log_2(\text{Fold-change})| \geq 1$. Then the DEGs were displayed in a volcano plot and a heatmap to visualize the changes in their expression levels. A Venn diagram was drawn to obtain the intersection of FRGs with DEGs and the genes of intersection were defined as FDEGs.

### Enrichment Analysis of FDEGs

All the FDEGs were uploaded to the Database for Annotation, Visualization, and Integrated Discovery (DAVID, https://david.ncifcrf.gov/summary.jsp) for Gene Ontology (GO) function and the Kyoto Encyclopedia of Gene and Genome (KEGG) functional pathway enrichment analyses. Then we visualized the top 10 enriched GO terms and KEGG pathways with the minimum $p$-value by the bubble diagrams.

### Hub Gene Identification

To show the relationship between these FDEGs, they were uploaded to the Search Tool for the Retrieval of Interacting Genes (http://string-db.org/) to construct a protein-protein interaction (PPI) network which was then visualized in the Cytoscape (https://www.cytoscape.org/). We used the plug-in Molecular Complex Detection to select the most closely connected module in which the degrees of genes were calculated by the degree algorithms of CytoHubba. Then we selected innovative genes in the module as hub genes.

### Hub Gene Analysis

The raw expression data of hub genes was extracted from the GSE8641 dataset, followed by the construction of a boxplot of the original expression data, a chordal graph showing the relationship between hub genes and the GO terms, and a scatter plot of the principal component analysis. The Gene Expression Profile Interactive Analysis database (http://gepia.cancer-pku.cn/) was used to draw the receiver operating characteristic (ROC) curves and the area under the ROC curve was calculated to evaluate the diagnostic values of hub genes. Then, the GSE100085

dataset was obtained from the GEO database. We conducted gene expression analysis and ROC curve analysis using the raw expression data of the target gene from the GSE100085.

## Prediction of Signaling Pathway

The co-expression genes of ATF4 were obtained from the COXPRESdb database (https://coxpresdb.jp) and the anxiety-related genes were downloaded from the GeneCards database (https://genecards.org). Common genes between them were acquired by a Venn diagram and these common genes were submitted to DAVID for KEGG pathway analysis. Then we visualized the KEGG pathways with the *p*-value < 0.05 by the bubble diagram.

## Establishment of the CRS-Induced Anxiety Mice Model

Male C57BL/6J mice (6-8-week-old, 18–20 g) were purchased from SPF (Beijing) Biotechnology Co., Ltd. (Beijing, China), and housed under standard laboratory conditions. All the following mouse experiments were approved by the Ethics Committee of The Second Affiliated Hospital of Guangzhou Medical University, and all procedures were conducted in accordance with the Guide for the Care and Use of Laboratory Animals.

To validate the expression level of hub genes, mice were randomly divided into Control and Anxiety groups. The mice in the Anxiety group were treated with daily 3 h restraint stress for 21 d to induce anxiety.[22,23] During the daily restraint stress experiment, the mice in the Anxiety group were located in 50 mL plastic tubes with a wall drilled with several vent holes to restrain major head and limb movement, with no access to food and water, and the mice in the Control group were placed in cages without food and water.[22,23] After the restraint stress, all mice had free access to food and water.[22,23] Additionally, after 21 d of CRS, mice were acclimated to a sound-attenuated testing room for 1 d before the behavior tests.

## Stereotaxic Microinjections of Lentivirus

Lentivirus harboring lentiviral vectors ATF4 (LV-oe-ATF4) and empty vectors (LV-oe-NC) were generated by GeneChem Co., Ltd. (Shanghai, China). Stereotaxic microinjections were conducted under sterile conditions. The mice were anesthetized with the inhalation anesthesia of 2% isoflurane and were then placed on a stereotactic frame. Lentiviral vectors ($2 \times 10^9$ transducing units/mL), empty vectors, or sterile saline were injected into the amygdala bilaterally (anterior-posterior, + 1.4 mm from meninges; medial-lateral, ± 0.34 mm; dorsal-ventral, − 4.8 mm) using a Hamilton microsyringe at a rate of 0.25 μL/min.[24,25] Each side was injected with 1 μL.[24] Two weeks after stereotaxic surgery, all mice except the Control group were treated with CRS to construct the anxiety model using the methods described above (Supplementary Figure 1). Therefore, to investigate the effect of ATF4 on anxiety disorders, the mice were divided into 4 groups: Control group (mice with injection of sterile saline and without CRS), CRS Anxiety group (mice with injection of sterile saline and CRS), CRS + LV-oe-ATF4 group (mice with injection of LV-oe-ATF4 and CRS), and CRS + LV-oe-NC group (mice with injection of empty vectors and CRS). Each group contained 6 mice. After 21 d of CRS, mice were acclimated to a sound-attenuated testing room for 1 d before the following behavior tests.

## Elevated Plus-Maze (EPM) Test

The EPM device was shaped with two opposing open (35 cm × 6 cm) and two opposing closed arms (35 cm × 6 cm) joined through a common central square (6 cm × 6 cm), which was placed 74 cm above the floor. Mice were put on the central square of the device, facing open arms, and allowed to move freely for 10 minutes.[23,26] Their behaviors were recorded by the SMART video tracking system and the total time spent in the open arms and the total number of entries into each open arm were calculated automatically by the software.[23,26]

## Forced Swimming Test (FST)

Mice were individually put in a cylinder (15 cm diameter, 25 cm height), unable to escape. The depth of water in the cylinder was 15 cm and the water temperature was maintained at 25 ± 1°C.[27] Each mouse was allowed to swim for 6 min and its duration of immobility during the last 4 min was recorded.[27]

## Light-Dark Box (LDB) Test

The box was divided into two separate compartments, a light compartment with white surfaces and a dark compartment with dark surfaces. Mice were individually placed in the center of the two compartments. Each mouse was allowed to move freely for 5 min.[27] During the test period, we recorded the time of each mouse staying in the light compartment and the number of transitions from the light to the dark compartment.[26,27]

## Open-Field Test (OFT)

At the start of the test, each mouse was placed in a corner of an open field to freely move for 6 min.[26] The mouse activity was recorded by the SMART video tracking system and the times to the central area were calculated automatically by the software.[26]

## Tail Suspension Test (TST)

We used adhesive tape to tie the tail of the mouse and thus suspended the mouse for 6 min.[27] Mice were considered to be immobile when they stopped moving limbs and bodies and only retained breathing. The accumulated immobility time during the last 4 min was recorded.[27]

## Collection of Samples and Histopathology Experiments

After behavioral tests, mice were anesthetized with the inhalation anesthesia of 2% isoflurane for collection of blood samples and then were sacrificed by cervical dislocation for collection of the brain samples. Then we rapidly isolated the hippocampi of the right brain samples on ice, which were used for the extraction of total RNAs and total proteins. The isolated hippocampi of the left brain samples were fixed in 4% paraformaldehyde for 48 h, which were then embedded in paraffin and sectioned (4 μm). Hematoxylin and eosin (H&E) staining was conducted to observe the neuronal structure and integrity of the hippocampus. After dewaxing in water, paraffin sections were stained with hematoxylin, differentiated with 1% hydrochloric acid alcohol for 10s, placed in water for 10 min, stained with eosin for 3 min, dehydrated, and sealed with neutral gum. Then the images were photographed with a microscope (Eclipse 80i, Tokyo, Japan). In addition, we conducted Nissl staining to evaluate the damage levels in the hippocampus. We dewaxed the paraffin sections and stained them with a cresyl violet staining solution (Solarbio, Beijing, China). After being washed, the sections were placed in Nissl differentiation solution, rapidly dehydrated, and sealed with neutral gum. Then the sections were left in the dark until the sealing reagent had dried and eventually photographed with a microscope (Eclipse 80i). The positive cell number of the Nissl body was calculated and analyzed by ImageJ software. The less positive number, the higher the level of damage was.

## Enzyme-Linked Immunosorbent Assay (ELISA)

Serum samples were obtained by centrifugation of the blood samples. We used corresponding ELISA kits (Esebio, Shanghai, China) to determine the content of corticosterone, 5-hydroxytryptamine (5-HT), glutamic acid (Glu), malondialdehyde (MDA), glutathione (GSH), and reactive oxygen species (ROS) in the serum of mice, in strict accordance with the instructions in the manual. Corticosterone, Glu, and 5-HT were anxiety-related indicators, while MDA, GSH, and ROS were detected to assess ferroptosis.

## Real-Time Quantitative Polymerase Chain Reaction (RT-qPCR)

The relative mRNA levels of hub genes were detected by RT-qPCR. Briefly, RNAs extracted from mice hippocampus samples, with an optical density at 260/280 between 1.9 and 2.0, were reverse transcribed into cDNAs which were applied for RT-qPCR on StepOnePlus Real-Time PCR System (Applied Biosystems, Foster City, CA, USA). The reaction conditions were set as follows: 95°C, 30s initial denaturation, and 40 amplification cycles (95°C, 10s, and 60°C, 30s). Supplementary Table 1 displayed the sequences of primers. The results were calculated using the $2^{-\Delta\Delta Ct}$ formula using β-actin as an internal standard.

## Western Blotting

Total proteins extracted from hippocampus samples were separated by 10% sodium dodecyl sulfate-polyacrylamide gel electrophoresis and transferred onto a polyvinylidene fluoride membrane (Millipore, Danvers, MA, USA), which was blocked with 5% skim milk and then incubated with primary antibodies at 4°C overnight. The primary antibodies included antibodies against ATF4 (ab216839; 1:1,000; Abcam, Cambridge, USA), ferritin heavy polypeptide 1 (FTH1; ab65080; 1:1,000; Abcam), transferrin receptor (TFRC; ab214039; 1:1,000; Abcam), glutathione peroxidase 4 (GPX4; ab125066; 1:2,000; Abcam), transforming growth factor beta1 (TGF-β1; ab215715; 1:1,000; Abcam), small mothers against decapentaplegic 3 (Smad3; ab208182; 1:1,000; Abcam), phospho-Smad3 (p-Smad3; ab52903; 1:2,000; Abcam), and β-actin (ab8227; 1:1,000; Abcam). The following day, the membrane after washing was incubated with a horseradish peroxidase-conjugated anti-rabbit secondary antibody (ab288151; 1:5,000; Abcam) for another 2 h. Finally, the protein exposure was conducted with a Tanon 5200 chemiluminescence imaging system (Tanon, Shanghai, China).

## Statistical Analysis

Data were presented as multiple groups of repeated data or means ± standard deviation and were processed by GraphPad Prism 7.0 statistical software (GraphPad, San Diego, CA, USA). The comparisons between two groups were determined by Student's *t*-test, and those among multiple groups were determined by one-way ANOVA with Tukey's post hoc analysis. A *p*-value less than 0.05 was considered statistically significant.

# Results

## DEGs Identification

We selected the original gene expression profiles of 6 anxiety samples and 6 control samples from the GSE8641 dataset and then conducted data correction and standardization shown in a boxplot (Figure 1A). After analysis of GEO2R, a total of 654 DEGs were identified, including 270 up-regulated and 384 down-regulated genes in anxiety samples in comparison to normal samples, which were visualized in a volcano plot (Figure 1B). We conducted a heatmap to visualize the top 15 up-regulated and down-regulated DEGs (Figure 1C), which were displayed in Supplementary Table 2. A total of 1317 FRGs were downloaded from the GeneCards database and 31 FDEGs were obtained after conducting a Venn diagram (Figure 1D), which were selected for GO and KEGG enrichment analyses. The GO terms and the top 10 KEGG pathways with the minimum *p*-value were shown with bubble plots (Figure 2A and B) and were listed in Supplementary Tables 3 and 4, respectively.

## PPI Network Construction and Hub Gene Selection

The PPI network of FDEGs was shown in Supplementary Figure 2A. We then imported the FDEGs into Cytoscape to identify a significant gene cluster by the plug-in Molecular Complex Detection (Supplementary Figure 2B) and obtain the degrees of genes in this cluster (Supplementary Figure 2C). According to the innovation, we selected pyruvate kinase M (PKM), ATF4, dihydrolipoamide dehydrogenase (DLD), mitogen-activated protein kinase kinase kinase 5 (MAP3K5), mechanistic target of rapamycin (mTOR), peroxiredoxin 2 (PRDX2), kirsten rat sarcoma viral oncogene homologue (KRAS), and HD domain containing 3 (HDDC3) as hub genes for the following analysis.

## Hub Gene Analysis

The boxplot showing the expression difference between the Control group and the Anxiety group was displayed in Figure 3A and the chordal graph exhibiting the correlation between hub genes and the GO terms was displayed in Figure 3B. A total of 2 principal component axes (PC1 and PC2) were generated after principal component analysis, which effectively explained 90.6% of the difference between the Control group and the Anxiety group (Figure 3C). The ROC curves showed that taking mTOR, PKM, ATF4, PRDX2, KRAS, or HDDC3 as an indicator, the true positive rates were all 100% in the GSE8641 dataset (Supplementary Figure 3), showing their effective diagnostic values in distinguishing anxiety from the control samples.
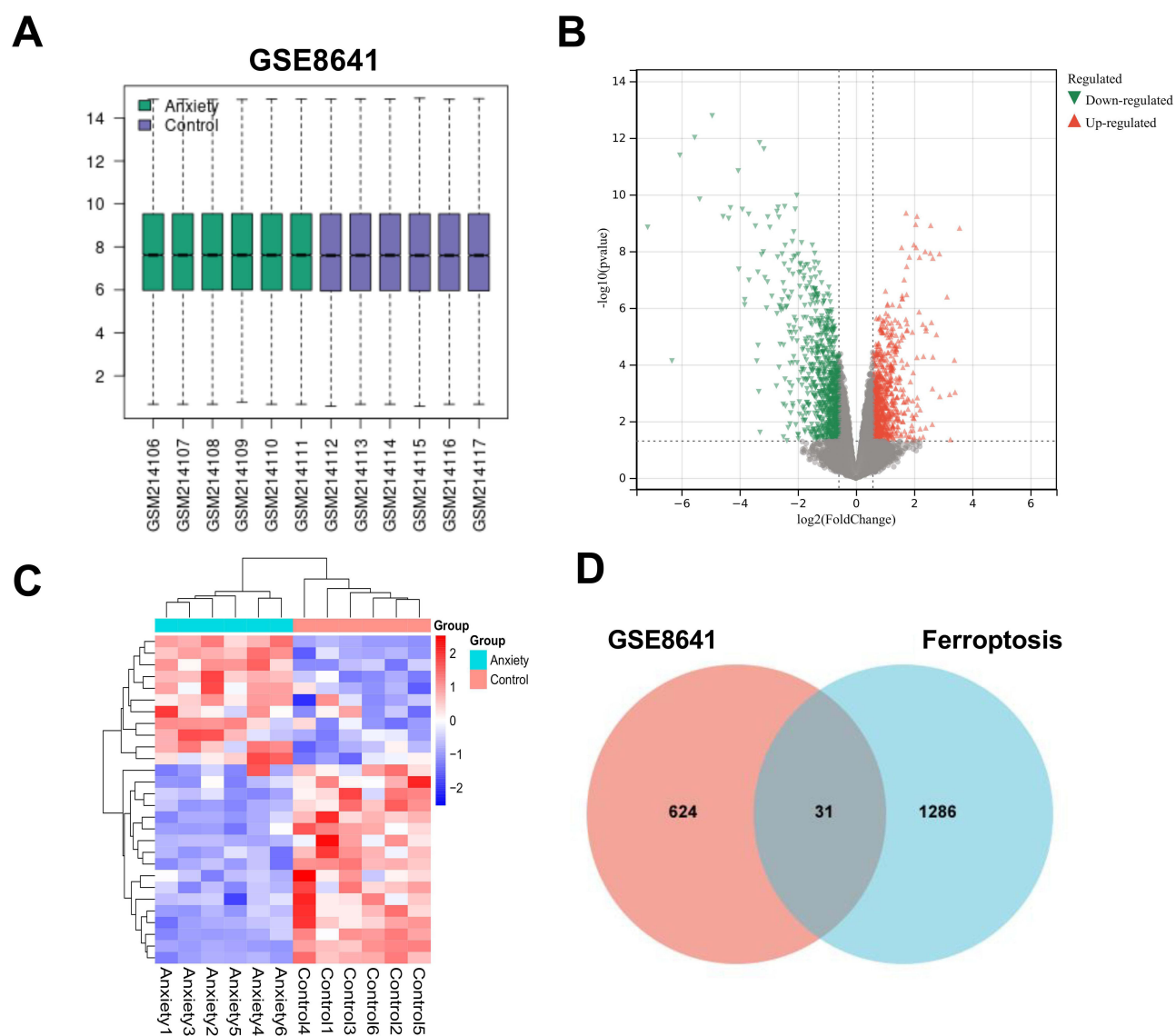
**Figure 1** Identification of differentially expressed genes (DEGs). (**A**) A box line plot showed the data correction results of the selected samples in GSE8641. (**B**) A volcano plot of DEGs in GSE8641. Red points presented up-regulated DEGs, and green points presented down-regulated DEGs. (**C**) A heatmap of DEGs in GSE8641. Red blocks presented up-regulated DEGs, and blue blocks presented down-regulated DEGs. (**D**) The Venn diagram of ferroptosis-related DEGs (FDEGs).

## Expression Analysis of Hub Genes on Anxiety Model Mice

We constructed anxiety model mice to verify the expression differences of hub genes via induction of CRS. Firstly, we assessed the histomorphology and the damage levels in the hippocampus. The images of H&E staining showed that the hippocampal neurons were arranged tightly and neatly in the Control group, while the cells were arranged loosely and disorderly with inflammatory cell infiltration in the Anxiety group (Figure 4A). Abundant visible Nissl bodies in the cytoplasm of hippocampal neurons were observed in the Control group, compared with which the positive cell number of Nissl body was significantly reduced in the Anxiety group ($p < 0.01$, Figure 4B), suggesting the hippocampal neurons were damaged. In the EPM test, compared with the Control group, mice in the Anxiety group spent less time in the open arms and had a reduced number of open-arm entries (all $p < 0.001$, Figure 4C-4D). In the FST, mice in the Anxiety group exhibited a longer immobility time during the last 4 min compared to the Control group ($p < 0.001$, Figure 4E). In the OFT, mice in the Anxiety group appeared less frequently in the central area and more frequently in the periphery ($p < 0.001$, Figure 5A and B). In addition, mice in the Anxiety group exhibited a longer immobility time in the TST, a reduced number of light-dark transitions, and less time spent in the light compartment in the LDB test (all $p < 0.001$,
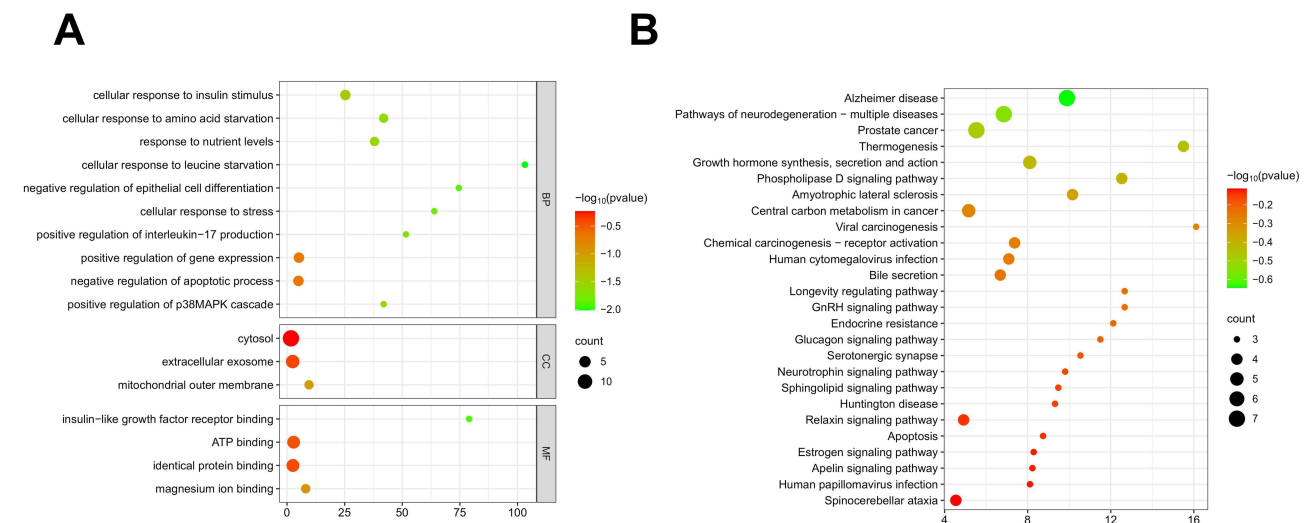
**Figure 2** Enrichment analysis of FDEGs. (**A**) A bubble diagram of the Gene Ontology (GO) enrichment analysis. (**B**) A bubble diagram of the Kyoto Encyclopedia of Genes and Genomes (KEGG) pathway analysis.
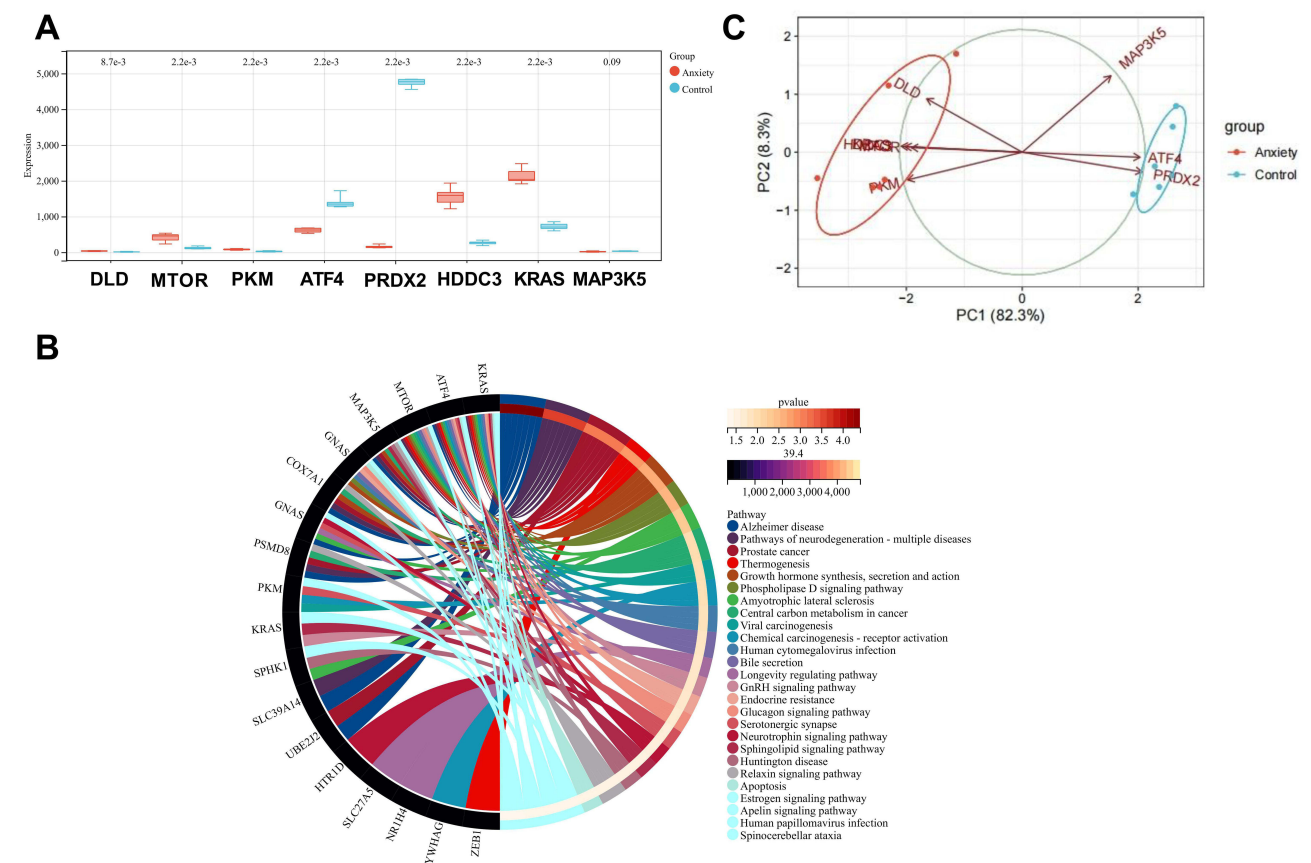


**Figure 3** Hub gene analysis. (**A**) A box line plot showed the expression difference of hub genes between the Control group and the Anxiety group in GSE8641. (**B**) A chordal graph with the expression changes of hub genes involved in the GO terms. (**C**) Principal component analysis of hub genes. The axes PC1 and PC2 in the figure were the first and second principal components. Dots represented samples, and different colors represented different groups.
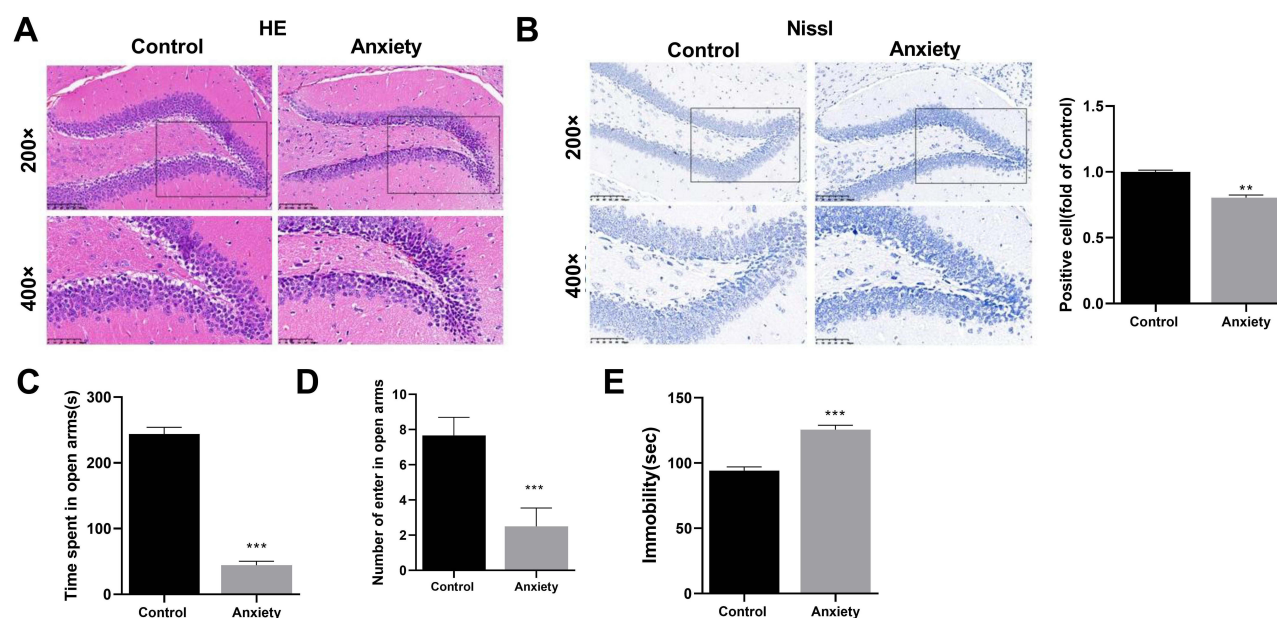
**Figure 4** Establishment of the CRS-induced anxiety mice model. (**A**) The representative images of hematoxylin-eosin staining (200×, scale bars=100 μm; 400×, scale bars=50 μm). (**B**) The representative images of Nissl staining (200×, scale bars=100 μm; 400×, scale bars=50 μm) and the quantitative results. (**C**) The time mice spent in open arms in the Elevated Plus-Maze (EPM) test. (**D**) The number of mice entered in open arms in the EPM test. (**E**) The immobile time in the forced swimming test (FST). ***$p < 0.001$, **$p < 0.01$ vs Control group.

Figure 4C and D). Lower levels of 5-HT and Glu and a higher level of corticosterone were determined in the serum of the Anxiety group (all $p < 0.001$, Figure 4E). The above results suggested that our modeling method was feasible. Then we detected the relative mRNA levels of hub genes in the hippocampus samples. Compared with the Control group, the relative mRNA levels of mTOR, PKM, DLD, HDDC3, and KRAS were significantly increased (all $p < 0.001$, Figure 5F), while ATF4 and PRDX2 were significantly down-regulated in the Anxiety group ($p < 0.001$ or $p < 0.01$, Figure 5F). The expression of MAP3K5 showed a decreasing trend in the Anxiety group, with no significant differences ($p > 0.05$, Figure 5F).

Based on the current level of research and innovation of each gene, we selected ATF4, the protein expression level of which was reduced in the Anxiety group ($p < 0.01$, Figure 5G), for further research. The GSE100085 dataset, including 4 anxiety and 4 control samples, was downloaded to validate the expression level and diagnostic value of ATF4. In GSE100085, ATF4 was significantly down-regulated in the Anxiety group compared with the Control group ($p < 0.05$, Supplementary Figure 4A), and the ROC curve showed that taking ATF4 as an indicator, the true positive rate was 100% (Supplementary Figure 4B) which suggested an effective diagnostic value, consistent with the previous results. Therefore, ATF4 was considered as the target gene for experimental validation.

## Overexpression of ATF4 Can Alleviate Anxiety-Like Behaviors in CRS-Induced Mice

Firstly, we detected the expression of ATF4 in each group. Compared with the Control group, the expression of ATF4 was down-regulated in the CRS-induced Anxiety group ($p < 0.001$, Figure 6A). Compared with the CRS + LV-oe-NC group, a higher ATF4 level was found in the CRS + LV-oe-ATF4 group ($p < 0.05$, Figure 6A). The images of H&E staining demonstrated that compared with the CRS + LV-oe-NC group, the hippocampal neurons were arranged more tightly, and the infiltration of inflammatory cells was improved in the CRS + LV-oe-ATF4 group (Figure 6B). The results of Nissl staining displayed an increased positive cell number of Nissl body in the CRS + LV-oe-ATF4 group compared to the CRS + LV-oe-NC group ($p < 0.01$, Figure 6C). Compared with the CRS + LV-oe-NC group, mice in the CRS + LV-oe -ATF4 group spent more time in the open arms and increased the number of open arm entries in the EPM test (all $p <$ 0.001, Figure 6D and E), and appeared more frequently in the central area and less frequently outside of the center in the OFT (all $p < 0.001$, Figure 7A and B). In the FST and TST, the immobility time was shorter in the CRS + LV-oe-ATF4
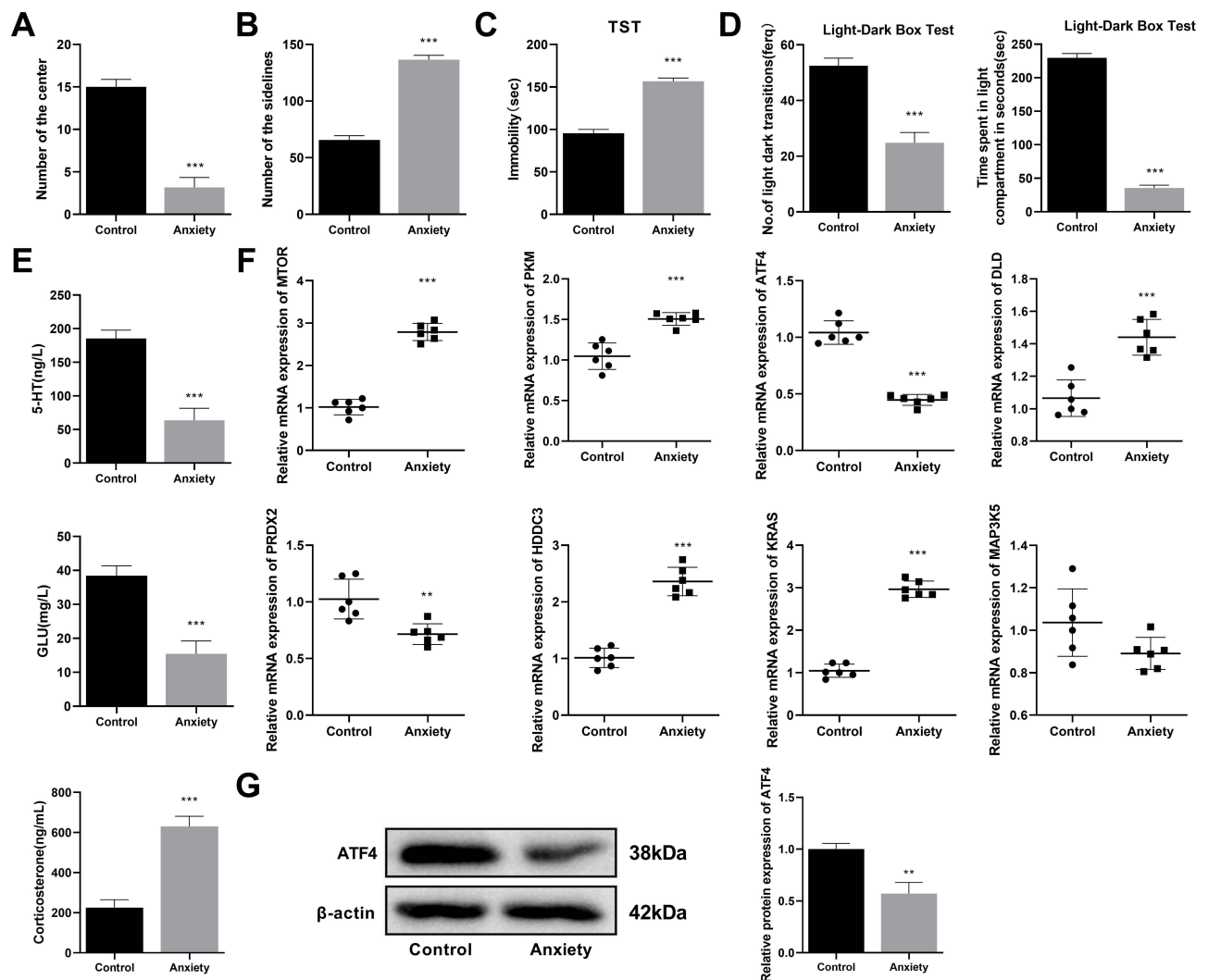
**Figure 5** Expression analysis of hub genes on anxiety model mice. (**A**) The frequency of mouse presence in the central region in the Open-field test (OFT). (**B**) The frequency of mouse appearance in the periphery in the OFT. (**C**) The immobile time in the tail suspension test (TST). (**D**) The number of mice entering the light compartment and the time mice spent in the light compartment during the Light-Dark box (LDB) test. (**E**) The content of corticosterone, 5-hydroxytryptamine, and glutamic acid. (**F**) The mRNA expression level of hub genes. (**G**) The protein expression level of activating transcription factor 4 (ATF4). ***$p < 0.001$, **$p < 0.01$ vs Control group.

group than in the CRS + LV-oe-NC group (all $p < 0.001$, Figure 7C and D). In the LDB test, the number of light-dark transitions and the time spent in the light compartment were both increased in the CRS + LV-oe-ATF4 group compared to the CRS + LV-oe-NC group (all $p < 0.001$, Figure 7E).

## Overexpression of ATF4 Inhibits CRS-Induced Ferroptosis of Hippocampal Neurons in Mice

The results of ELISA and Western blotting exhibited that the expression levels of MDA, ROS, and TFRC were significantly elevated and GSH, GPX4, and FTH1 were decreased in the CRS-induced Anxiety group compared to the Control group ($p < 0.001$ or $p < 0.01$, Figure 7F and G), demonstrating that CRS promoted ferroptosis of hippocampal neurons in mice. After overexpressing ATF4, we observed higher expression levels of GSH, GPX4, and FTH1 and lower expression levels of MDA, ROS, and TFRC in the CRS + LV-oe-ATF4 group compared to the CRS + LV-oe-NC group ($p < 0.001$ or $p < 0.01$ or $p < 0.05$, Figure 7F and G), suggesting that ATF4 overexpression may improve hippocampal tissue damage via suppression of CRS-induced ferroptosis of hippocampal neurons.
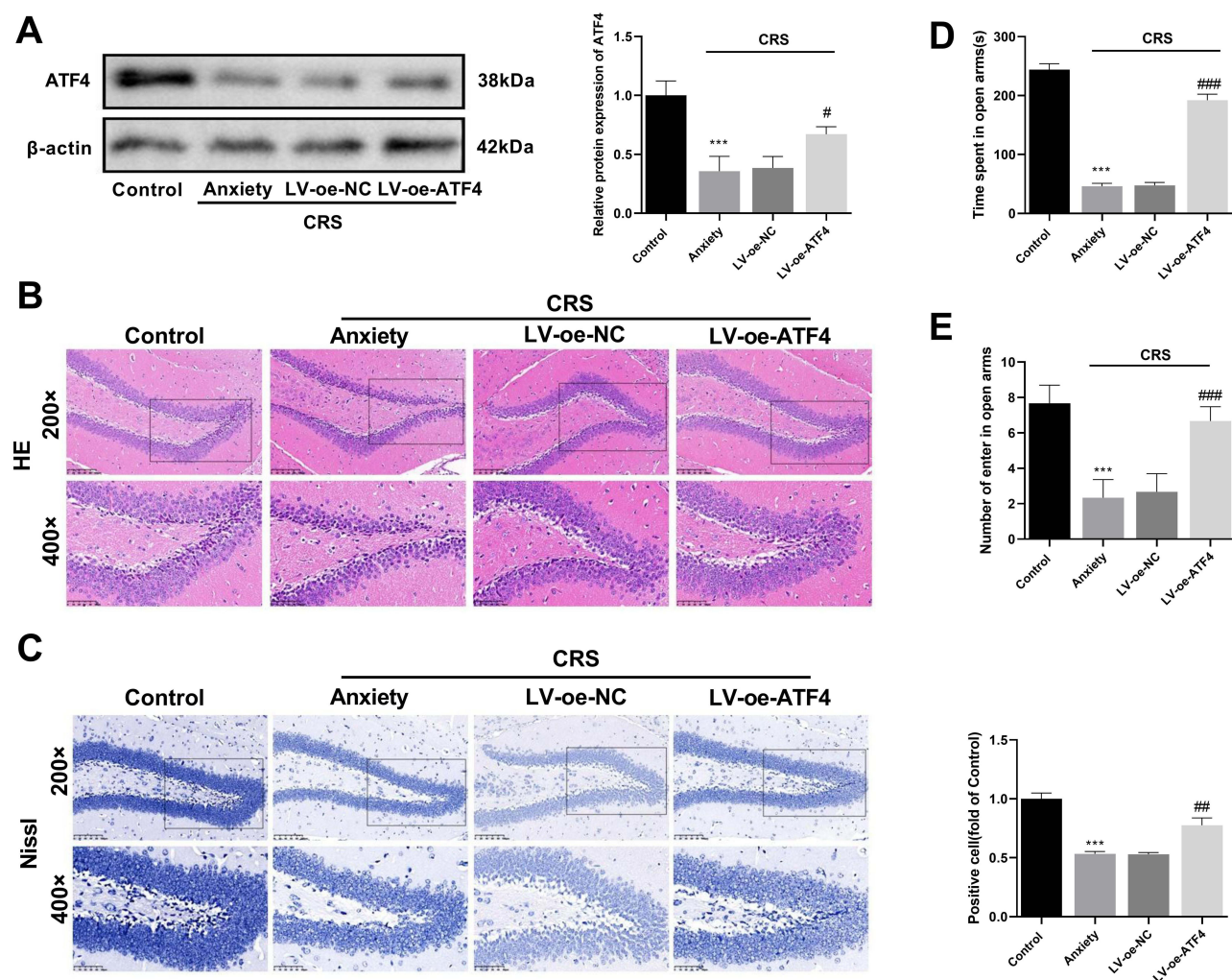
**Figure 6** Overexpression of ATF4 improved CRS-induced hippocampal tissue damage. (A) The protein expression level of ATF4. (B) The representative images of hematoxylin-eosin staining (200×, scale bars=100 μm; 400×, scale bars=50 μm). (C) The representative images of Nissl staining (200×, scale bars=100 μm; 400×, scale bars=50 μm) and the quantitative results. (D) The time mice spent in open arms in the EPM test. (E) The number of mice entering in open arms in the EPM test. ***$p < 0.001$ vs Control group; ####$p < 0.001$, ##$p < 0.01$, #$p < 0.05$ vs CRS + LV-oe-NC group.

## ATF4 Overexpression Activates the TGF-β Signaling Pathway

To uncover the promising regulatory mechanism of ATF4, the possible signaling pathway of ATF4 was predicted and verified. A total of 6855 anxiety-related genes and 1000 genes co-expressed with ATF4 were downloaded and then 243 genes of intersection were obtained after construction of a Venn diagram (Figure 8A). Then we submitted these genes for KEGG pathway enrichment analysis and selected the TGF-β signaling pathway for verification based on the current level of research (Figure 8B). The expression levels of TGF-β1, Smad3, and p-Smad3 were determined by Western blotting. The results showed that the TGF-β signaling pathway was repressed after CRS treatment based on the down-regulation of TGF-β1 and p-Smad3/Smad3 ($p < 0.01$ or $p < 0.001$, Figure 8C), whereas ATF4 overexpression stimulated the TGF-β signal via enhancing the levels of TGF-β1 and p-Smad3/Smad3 ($p <0.05$ or $p < 0.001$, Figure 8C).

## Discussion

Anxiety disorders seriously affect patients' mental health and quality of life, with limited effectiveness of current treatments.[28] Therefore, exploring a novel therapeutic target for anxiety disorders has an important significance. In this research, we obtained 8 ferroptosis-related hub genes in the anxiety-related database after bioinformatics analysis and selected ATF4 for experimental verification. The results exhibited that overexpression of ATF4 could relieve CRS-
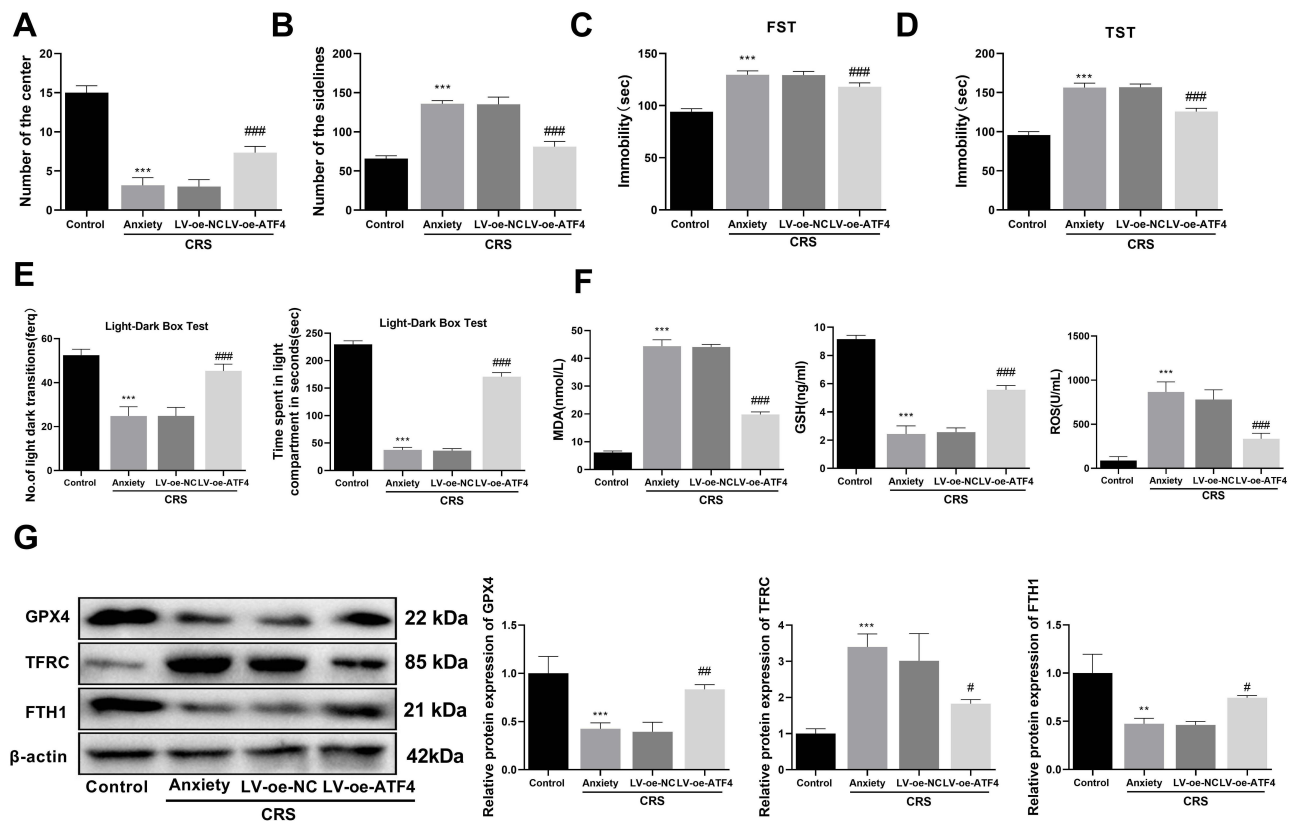
**Figure 7** Overexpression of ATF4 improved CRS-induced anxiety-like behaviors and inhibited ferroptosis. (**A**) The frequency of mouse presence in the central region in the OFT. (**B**) The frequency of mouse appearance in the periphery in the OFT. (**C**) The immobile time in the FST. (**D**)The immobile time in the TST. (**E**) The number of mice entering the light compartment and the time mice spent in the light compartment during the LDB test. (**F**) Content detection of malondialdehyde, glutathione, and reactive oxygen. (**G**) The protein expression level of ferritin heavy polypeptide 1, transferrin receptor, and glutathione peroxidase 4. ***$p < 0.001$, **$p < 0.01$ vs Control group; ###$p < 0.001$, ##$p < 0.01$, #$p < 0.05$ vs CRS + LV-oe-NC group.

induced anxiety-like behaviors and hippocampal damage in mice, and inhibit ferroptosis by activating the TGF-β signaling pathway.

Bioinformatics analysis is an important tool for searching for promising therapeutic targets of diseases,[26] based on which we obtained 8 hub genes of anxiety in this study, namely PKM, DLD, MAP3K5, mTOR, PRDX2, KRAS, HDDC3, and ATF4. Vakhitova et al have reported that PKM is involved in the mechanisms of action of the anxiolytic effect of fabomotizole.[29] Suppression of mTOR signaling has been reported to aggravate anxiety-like behaviors in mice.[30] Early-life stress impairs synaptic plasticity and aggravates anxiety-like and cognition-related behaviors by repressing the mTOR signaling in the hippocampus.[31] McCoy et al have found that exposure to maternal separation exhibits the anxiolytic effect in rats by decreasing methylation at sites within MAP3K5.[32] The role of ATF4, DLD, PRDX2, KRAS, and HDDC3 in anxiety remains unclear. However, ATF4 has been found to be related to different kinds of mental diseases,[33,34] which provides the possibility for ATF4 to exert an anxiolytic effect. In our study, we found ATF4 was down-regulated in anxiety samples and over-expression of ATF4 could improve the CRS-induced anxiety-like behaviors in mice.

The hippocampus is an essential brain area in modulating the progression of mental diseases[35] and emotional behaviors,[36,37] including anxiety reactions.[38] Increased evidence has found that hippocampal damage is one of the causes of the development of anxiety. Chronic unpredictable stress induces anxiety-like behaviors by promoting myelin damage in the hippocampal formation.[39] Alpha-ketoglutarate is able to improve anxiety-like behaviors by reducing hippocampal synaptic damage, with up-regulation of gephyrin-related genes.[40] Interleukin-17A causes epilepsy-induced anxiety by promoting hippocampal damage.[41] Raper et al have found that damage to the hippocampus increases anxiety-like behaviors in monkeys.[42] Ferroptosis plays a role in inducing damage to the hippocampus. Lv et al have reported that maternal sleep deprivation activates ferroptosis in offspring rats to cause hippocampal neuroinflammation damage, leading to cognitive
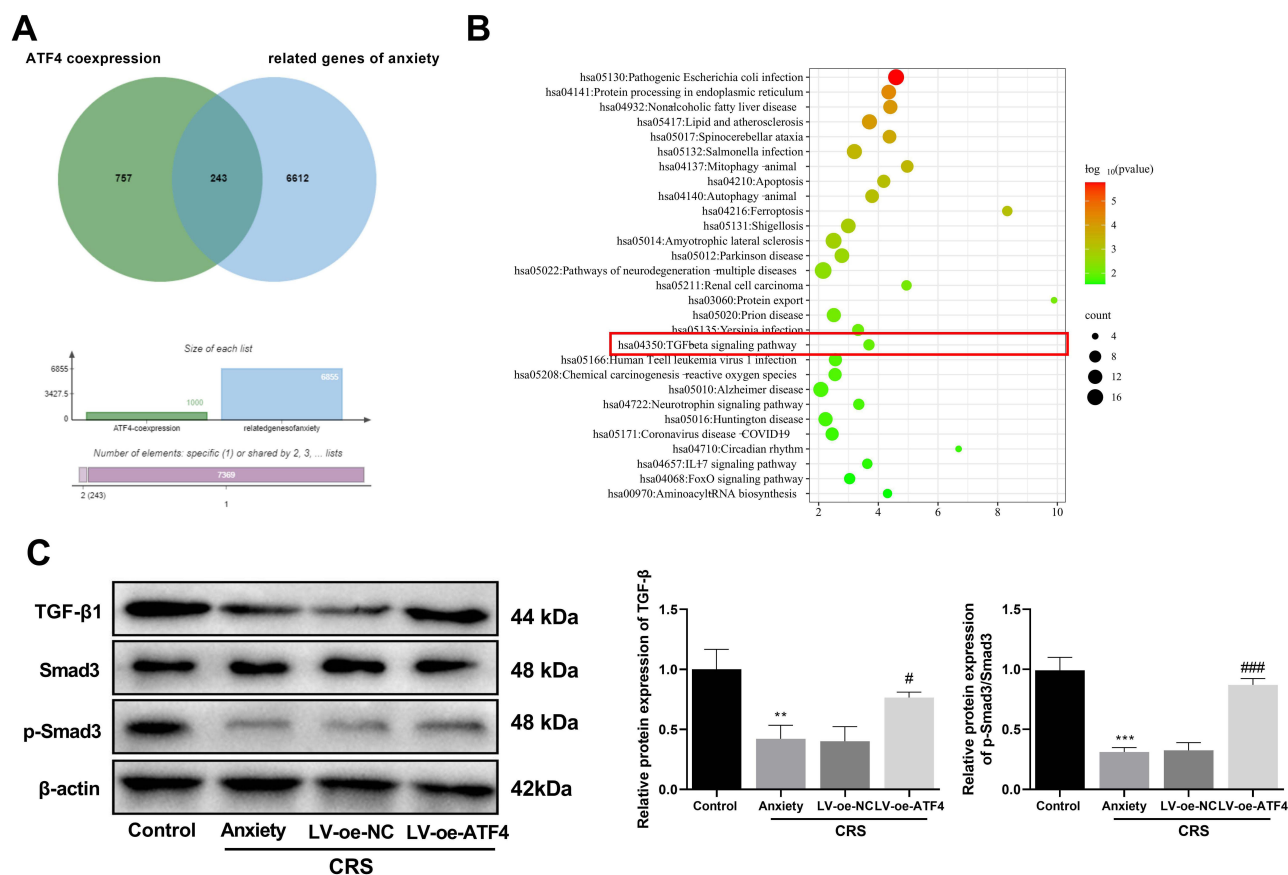
**Figure 8** ATF4 overexpression activated the TGF-β signaling pathway. (**A**) A Venn diagram of co-expressed genes with ATF4 and anxiety-related genes. (**B**) A bubble plot of KEGG enrichment analysis. (**C**) The expression level of transforming growth factor beta1 and p-Smad/Smad was detected by Western blotting. ***$p < 0.001$, **$p < 0.01$ vs Control group; ###$p < 0.001$, #$p < 0.05$ vs CRS + LV-oe-NC group.

impairment.[43] Inhibition of ferroptosis can alleviate kainic acid-induced hippocampal neuron damage and cognitive impairment.[44] In neonatal rats, down-regulation of toll-like receptor 4 suppresses hypoxia-ischemia-induced hippocampal damage via the inhibition of ferroptosis.[45] In this study, we found that up-regulation of ATF4 could improve CRS-induced hippocampal tissue damage and suppress ferroptosis of hippocampal neurons in mice, suggesting that the anxiolytic effect of ATF4 overexpression may be associated with the alleviation of hippocampal damage by inhibiting ferroptosis.

Smad-mediated TGF-β signaling is considered as the canonical TGF-β signaling pathway.[46] More and more studies have reported the relationship between this pathway and ATF4. For instance, TGF-β increases the activation of ATF4 to promote metabolic reprogramming in lung fibroblasts.[47] In pancreatic cancer, up-regulation of ATF4 facilitates malignancy and gemcitabine resistance by triggering the TGF-β signaling pathway.[48] Vanhoutte et al have observed that the TGF-β signaling pathway stimulates the expression of ATF4 to promote the activation of autophagy and the ubiquitin-proteasome system, leading to muscle atrophy.[49] In triple-negative breast cancer, ATF4 suppression inhibits tumor growth and metastases via the TGF-β signaling pathway.[50] In addition, this pathway has been found to be involved in regulating ferroptosis in some disease models. In hepatocellular carcinoma, the protein inhibitor of activated signal transducer and activator of transcription 3 stimulates the TGF-β signaling pathway by interacting with Smad2/3 to promote ferroptosis, exerting its anti-tumor effect.[51] Hepatocyte growth factor plays a role in alleviating silicosis fibrosis by inhibiting ferroptosis of lung tissue via the suppression of the TGF-β signaling pathway.[52] In this research, ATF4 up-regulation elevated the protein expression levels of TGF-β1 and p-Smad3/Smad3 in hippocampal neurons of mice, suggesting the activation of the TGF-β signaling pathway may be the underlying regulatory mechanism of ATF4 alleviating anxiety and regulating ferroptosis.

There are also some limitations to this study. First, it is an indirect conclusion that ATF4 overexpression represses ferroptosis to suppress anxiety by activating the TGF-β signaling pathway, and it needs to be verified by the TGF-β signaling pathway antagonist and agonist in the future. The direct regulatory relationship and the exact molecular interactions between ATF4 and the TGF-β signaling pathway in anxiety need to be further investigated. Second, our results were obtained only through animal experiments and limited to mice models. More experiments are needed to explore how to translate our findings into clinical applications.

To summarize, ATF4 was screened out as a ferroptosis-related anxiolytic gene after bioinformatics analysis, and overexpressing ATF4 in vivo could improve the CRS-induced anxiety-like behaviors and hippocampal damage, with the suppression of ferroptosis and the activation of the TGF-β signaling pathway. Our results showed a protective effect of ATF4 on anxiety disorders, suggesting that ATF4 could be a therapeutic target for anxiety disorders.

## Data Sharing Statement
The data that support the findings of this study are openly available in Gene Expression Omnibus at https://www.ncbi.nlm.nih.gov/geo/, reference number GSE8641.

## Ethics Approval and Consent to Participate
The animal experiments were approved by the Ethics Committee of The Second Affiliated Hospital of Guangzhou Medical University, and all procedures were conducted in accordance with the Guide for the Care and Use of Laboratory Animals. Since our experiment did not involve human clinical research, only using anxiety model mice and public data derived from mouse muscle, human ethical approval was not required.

## Author Contributions
All authors made a significant contribution to the work reported, whether that is in the conception, study design, execution, acquisition of data, analysis, and interpretation, or in all these areas; took part in drafting, revising, or critically reviewing the article; gave final approval of the version to be published; have agreed on the journal to which the article has been submitted; and agree to be accountable for all aspects of the work.

## Disclosure
The authors declare that they have no conflicts of interest in this work.

## References
1. Huang Y, Wang Y, Wang H, et al. Prevalence of mental disorders in China: A cross-sectional epidemiological study. *Lancet Psychiatry*. 2019;6 (3):211–224. doi:10.1016/s2215-0366(18)30511-x
2. Nyberg J, Henriksson M, Wall A, et al. Anxiety severity and cognitive function in primary care patients with anxiety disorder: a cross-sectional study. *BMC Psychiatry*. 2021;21(1):617. doi:10.1186/s12888-021-03618-z
3. DeMartini J, Patel G, Fancher TL. Generalized Anxiety Disorder. *Ann Intern Med*. 2019;170(7):Itc49–itc64. doi:10.7326/aitc201904020
4. Global. regional, and national burden of 12 mental disorders in 204 countries and territories, 1990-2019: a systematic analysis for the Global Burden of Disease Study 2019. *Lancet Psychiatry*. 2022;9(2):137–150. doi:10.1016/s2215-0366(21)00395-3
5. Cuijpers P, Gentili C, Banos RM, et al. Relative effects of cognitive and behavioral therapies on generalized anxiety disorder, social anxiety disorder and panic disorder: a meta-analysis. *J Anxiety Disord*. 2016;43:79–89. doi:10.1016/j.janxdis.2016.09.003
6. Lei G, Zhuang L, Gan B. Targeting ferroptosis as a vulnerability in cancer. *Nat Rev Cancer*. 2022;22(7):381–396. doi:10.1038/s41568-022-00459-0
7. Tang D, Chen X, Kang R, et al. Ferroptosis: molecular mechanisms and health implications. *Cell Res*. 2021;31(2):107–125. doi:10.1038/s41422-020-00441-1
8. Xu C, Xiong Q, Tian X, et al. Alcohol Exposure Induces Depressive and Anxiety-like Behaviors via Activating Ferroptosis in Mice. *Int J Mol Sci*. 2022;23(22). doi:10.3390/ijms232213828

9. Mao L, You J, Xie M, et al. Arginine Methylation of β-Catenin Induced by PRMT2 Aggravates LPS-Induced Cognitive Dysfunction and Depression-Like Behaviors by Promoting Ferroptosis. *Mol Neurobiol*. 2024. doi:10.1007/s12035-024-04019-5

10. Wang Y, Wang S, Xin Y, et al. Hydrogen sulfide alleviates the anxiety-like and depressive-like behaviors of type 1 diabetic mice via inhibiting inflammation and ferroptosis. *Life Sci*. 2021;278:119551. doi:10.1016/j.lfs.2021.119551

11. Tang H, Kang R, Liu J, et al. ATF4 in cellular stress, ferroptosis, and cancer. *Arch Toxicol*. 2024;98(4):1025–1041. doi:10.1007/s00204-024-03681-x

12. He F, Zhang P, Liu J, et al. ATF4 suppresses hepatocarcinogenesis by inducing SLC7A11 (xCT) to block stress-related ferroptosis. *J Hepatol*. 2023;79(2):362–377. doi:10.1016/j.jhep.2023.03.016

13. Gao R, Kalathur RKR, Coto-Llerena M, et al. YAP/TAZ and ATF4 drive resistance to Sorafenib in hepatocellular carcinoma by preventing ferroptosis. *EMBO Mol Med*. 2021;13(12):e14351. doi:10.15252/emmm.202114351

14. Mukherjee D, Chakraborty S, Bercz L, et al. Tomatidine targets ATF4-dependent signaling and induces ferroptosis to limit pancreatic cancer progression. *iScience*. 2023;26(8):107408. doi:10.1016/j.isci.2023.107408

15. Chen D, Fan Z, Rauh M, et al. ATF4 promotes angiogenesis and neuronal cell death and confers ferroptosis in a xCT-dependent manner. *Oncogene*. 2017;36(40):5593–5608. doi:10.1038/onc.2017.146

16. Wang Y, Zhao Y, Ye T, et al. Ferroptosis Signaling and Regulators in Atherosclerosis. *Front Cell Dev Biol*. 2021;9:809457. doi:10.3389/fcell.2021.809457

17. Ham S, Kim JH, Kim H, et al. ATF4-activated parkin induction contributes to deferasirox-mediated cytoprotection in Parkinson's disease. *Toxicol Res*. 2023;39(2):191–199. doi:10.1007/s43188-022-00157-x

18. Wei N, Zhu LQ, Liu D. ATF4: a Novel Potential Therapeutic Target for Alzheimer's Disease. *Mol Neurobiol*. 2015;52(3):1765–1770. doi:10.1007/s12035-014-8970-8

19. Yuan F, Zhou Z, Wu S, et al. Intestinal activating transcription factor 4 regulates stress-related behavioral alterations via paraventricular thalamus in male mice. *Proc Natl Acad Sci U S A*. 2023;120(19):e2215590120. doi:10.1073/pnas.2215590120

20. Corona C, Pasini S, Liu J, et al. Activating Transcription Factor 4 (ATF4) Regulates Neuronal Activity by Controlling GABA(B)R Trafficking. *J Neurosci*. 2018;38(27):6102–6113. doi:10.1523/jneurosci.3350-17.2018

21. Pasini S, Corona C, Liu J, et al. Specific downregulation of hippocampal ATF4 reveals a necessary role in synaptic plasticity and memory. *Cell Rep*. 2015;11(2):183–191. doi:10.1016/j.celrep.2015.03.025

22. Hosseini F, Khakpai F, Fazli-Tabaei S, et al. Interaction between citalopram and omega-3 fatty acids on anxiety and depression behaviors and maintaining the stability of brain pyramidal neurons in mice. *Neurosci Lett*. 2024;824:137688. doi:10.1016/j.neulet.2024.137688

23. Lyu Y, Wei X, Yang X, et al. 11-Ethoxyviburtinal improves chronic restraint stress-induced anxiety-like behaviors in gender-specific mice via PI3K/Akt and E(2) /ERβ signaling pathways. *Phytother Res*. 2023;37(9):4149–4165. doi:10.1002/ptr.7876

24. Wang J, Yang Y, Liu J, et al. Loss of sodium leak channel (NALCN) in the ventral dentate gyrus impairs neuronal activity of the glutamatergic neurons for inflammation-induced depression in male mice. *Brain Behav Immun*. 2023;110:13–29. doi:10.1016/j.bbi.2023.02.013

25. Li RM, Xiao L, Zhang T, et al. Overexpression of fibroblast growth factor 13 ameliorates amyloid-β-induced neuronal damage. *Neural Regen Res*. 2023;18(6):1347–1353. doi:10.4103/1673-5374.357902

26. Liu H, Huang X, Li Y, et al. TNF signaling pathway-mediated microglial activation in the PFC underlies acute paradoxical sleep deprivation-induced anxiety-like behaviors in mice. *Brain Behav Immun*. 2022;100:254–266. doi:10.1016/j.bbi.2021.12.006

27. Du Y, Xu CL, Yu J, et al. HMGB1 in the mPFC governs comorbid anxiety in neuropathic pain. *J Headache Pain*. 2022;23(1):102. doi:10.1186/s10194-022-01475-z

28. Kowalchuk A, Gonzalez SJ, Zoorob RJ. Anxiety Disorders in Children and Adolescents. *Am Fam Physician*. 2022;106(6):657–664.

29. Vakhitova YV, Kuzmina US, Voronin MV, et al. Effect of Fabomotizole on Brain Gene Expression in MR Rats in the Open Field Test. *Dokl Biochem Biophys*. 2019;488(1):313–315. doi:10.1134/s1607672919050090

30. Koehl M, Ladevèze E, Catania C, et al. Inhibition of mTOR signaling by genetic removal of p70 S6 kinase 1 increases anxiety-like behavior in mice. *Transl Psychiatry*. 2021;11(1):165. doi:10.1038/s41398-020-01187-5

31. Wang A, Zou X, Wu J, et al. Early-Life Stress Alters Synaptic Plasticity and mTOR Signaling: correlation With Anxiety-Like and Cognition-Related Behavior. *Front Genet*. 2020;11:590068. doi:10.3389/fgene.2020.590068

32. McCoy CR, Rana S, Stringfellow A, et al. Neonatal maternal separation stress elicits lasting DNA methylation changes in the hippocampus of stress-reactive Wistar Kyoto rats. *Eur J Neurosci*. 2016;44(10):2829–2845. doi:10.1111/ejn.13404

33. Kumar A, Karuppagounder SS, Chen Y, et al. 2-Deoxyglucose drives plasticity via an adaptive ER stress-ATF4 pathway and elicits stroke recovery and Alzheimer's resilience. *Neuron*. 2023;111(18):2831–2846.e10. doi:10.1016/j.neuron.2023.06.013

34. Yang T, Zhang Y, Chen L, et al. The potential roles of ATF family in the treatment of Alzheimer's disease. *Biomed Pharmacother*. 2023;161:114544. doi:10.1016/j.biopha.2023.114544

35. Ghasemi M, Navidhamidi M, Rezaei F, et al. Anxiety and hippocampal neuronal activity: relationship and potential mechanisms. *Cogn Affect Behav Neurosci*. 2022;22(3):431–449. doi:10.3758/s13415-021-00973-y

36. Cameron HA, Glover LR. Adult neurogenesis: beyond learning and memory. *Annu Rev Psychol*. 2015;66:53–81. doi:10.1146/annurev-psych-010814-015006

37. Price RB, Duman R. Neuroplasticity in cognitive and psychological mechanisms of depression: an integrative model. *Mol Psychi*. 2020;25(3):530–543. doi:10.1038/s41380-019-0615-x

38. Bartlett AA, Singh R, Hunter RG. Anxiety and Epigenetics. *Adv Exp Med Biol*. 2017;978:145–166. doi:10.1007/978-3-319-53889-1_8

39. Huang CX, Xiao Q, Zhang L, et al. Stress-induced myelin damage in the hippocampal formation in a rat model of depression. *J Psychiatr Res*. 2022;155:401–409. doi:10.1016/j.jpsychires.2022.09.025

40. Wang B, Zhao T, Chen XX, et al. Gestational 1-nitropyrene exposure causes anxiety-like behavior partially by altering hippocampal epigenetic reprogramming of synaptic plasticity in male adult offspring. *J Hazard Mater*. 2023;453:131427. doi:10.1016/j.jhazmat.2023.131427

41. Choi IY, Cho ML, Cho KO. Interleukin-17A Mediates Hippocampal Damage and Aberrant Neurogenesis Contributing to Epilepsy-Associated Anxiety. *Front Mol Neurosci*. 2022;15:917598. doi:10.3389/fnmol.2022.917598

42. Raper J, Wilson M, Sanchez M, et al. Increased anxiety-like behaviors, but blunted cortisol stress response after neonatal hippocampal lesions in monkeys. *Psychoneuroendocrinology*. 2017;76:57–66. doi:10.1016/j.psyneuen.2016.11.018

43. Lv J, Xu S, Meng C, et al. Ferroptosis participated in hippocampal neuroinflammation damage of in offspring rats after maternal sleep deprivation. *J Neuroimmunol*. 2023;375:578021. doi:10.1016/j.jneuroim.2023.578021

44. Ye Q, Zeng C, Luo C, et al. Ferrostatin-1 mitigates cognitive impairment of epileptic rats by inhibiting P38 MAPK activation. *Epilepsy Behav*. 2020;103(Pt A):106670. doi:10.1016/j.yebeh.2019.106670

45. Zhu K, Zhu X, Sun S, et al. Inhibition of TLR4 prevents hippocampal hypoxic-ischemic injury by regulating ferroptosis in neonatal rats. *Exp Neurol*. 2021;345:113828. doi:10.1016/j.expneurol.2021.113828

46. Hiew LF, Poon CH, You HZ, et al. TGF-β/Smad Signalling in Neurogenesis: implications for Neuropsychiatric Diseases. *Cells*. 2021;10(6). doi:10.3390/cells10061382

47. O'Leary EM, Tian Y, Nigdelioglu R, et al. TGF-β Promotes Metabolic Reprogramming in Lung Fibroblasts via mTORC1-dependent ATF4 Activation. *Am J Respir Cell Mol Biol*. 2020;63(5):601–612. doi:10.1165/rcmb.2020-0143OC

48. Wei L, Lin Q, Lu Y, et al. Cancer-associated fibroblasts-mediated ATF4 expression promotes malignancy and gemcitabine resistance in pancreatic cancer via the TGF-β1/SMAD2/3 pathway and ABCC1 transactivation. *Cell Death Dis*. 2021;12(4):334. doi:10.1038/s41419-021-03574-2

49. Vanhoutte D, Schips TG, Minerath RA, et al. Thbs1 regulates skeletal muscle mass in a TGFβ-Smad2/3-ATF-dependent manner. *Cell Rep*. 2024;43(5):114149. doi:10.1016/j.celrep.2024.114149

50. González-González A, Muñoz-Muela E, Marchal JA, et al. Activating Transcription Factor 4 Modulates TGFβ-Induced Aggressiveness in Triple-Negative Breast Cancer via SMAD2/3/4 and mTORC2 Signaling. *Clin Cancer Res*. 2018;24(22):5697–5709. doi:10.1158/1078-0432.Ccr-17-3125

51. Bao W, Wang J, Fan K, et al. PIAS3 promotes ferroptosis by regulating TXNIP via TGF-β signaling pathway in hepatocellular carcinoma. *Pharmacol Res*. 2023;196:106915. doi:10.1016/j.phrs.2023.106915

52. Bao R, Wang Q, Yu M, et al. AAV9-HGF cooperating with TGF-beta/Smad inhibitor attenuates silicosis fibrosis via inhibiting ferroptosis. *Biomed Pharmacother*. 2023;161:114537. doi:10.1016/j.biopha.2023.114537